JOURNAL OF VIROLOGY, Oct. 1996, p. 6576–6588 Vol. 70, No. 10
0022-538X/96/$04.00+0

Cellular Origin and Ultrastructure of Membranes Induced during Poliovirus Infection

ANDREAS SCHLEGEL,[1,2]† THOMAS H. GIDDINGS, JR.,[1] MARK S. LADINSKY,[1] AND KARLA KIRKEGAARD[1,2]*

Department of Molecular, Cellular and Developmental Biology,[1] and Howard Hughes Medical Institute,[2] University of Colorado, Boulder, Colorado 80309

Received 2 February 1996/Accepted 8 June 1996

Poliovirus RNA replicative complexes are associated with cytoplasmic membranous structures that accumulate during viral infection. These membranes were immunoisolated by using a monoclonal antibody against the viral nonstructural protein 2C. Biochemical analysis of the isolated membranes revealed that several organelles of the host cell (lysosomes, *trans*-Golgi stack and *trans*-Golgi network, and endoplasmic reticulum) contributed to the virus-induced membranous structures. Electron microscopy of infected cells preserved by high-pressure freezing revealed that the virus-induced membranes contain double lipid bilayers that surround apparently cytosolic material. Immunolabeling experiments showed that poliovirus proteins 2C and 3D were localized to the same membranes as the cellular markers tested. The morphological and biochemical data are consistent with the hypothesis that autophagy or a similar host process is involved in the formation of the poliovirus-induced membranes.

Poliovirus and other picornaviruses are nonenveloped icosahedral viruses whose RNA genomes are translated, replicated, and packaged in the cytoplasm of infected primate cells. Dramatic morphological and biochemical alterations in the host cell accompany virus infection (reviewed in references 61 and 62). Cellular translation (30), transcription (17–19), and protein secretion (25) are inhibited. During the course of poliovirus infection, intracellular calcium concentrations increase greatly (44) and lysosomal enzymes redistribute into the cytosol (39). Starting at approximately 2 h postinfection, membranous structures begin to accumulate in the cytoplasm of poliovirus-infected cells; these structures were described 30 years ago by Dales et al. as small, membrane-enclosed bodies (21) that range from 50 to 400 nm in size (16).

RNA-dependent RNA synthesis by all eukaryotic positive-strand RNA viruses tested to date occurs in association with cytoplasmic membranes. Several other picornaviruses such as coxsackieviruses (46), echoviruses (34, 35, 65), mengovirus (2, 3), and encephalomyocarditis virus (22) induce the rearrangement of intracellular membranes. In addition, alphavirus RNA replication complexes are found on the surfaces of membranous vesicles that have been identified as endosomal in origin (32). RNA replication complexes from flock house virus, a nodavirus, can be isolated only in association with membranes of unknown origin from infected insect cells; in vitro RNA synthesis by these complexes is stimulated by glycerolphospholipid (75). Reticular inclusions seen in coronavirus-infected cells may be involved in viral RNA synthesis; in some images, these membranous structures appear to have double membranes (26). The mechanisms of membrane proliferation and of assembly of the RNA synthetic complexes for these viruses are unknown. The extensive association of RNA replication with intracellular membranes is especially noteworthy for picornaviruses and other nonenveloped viruses, since cellular membranes form no part of the mature virion structure. Nonetheless, newly synthesized poliovirus RNA (72), poliovirus proteins known to be required for RNA replication (7, 9, 10, 69, 72), and virus particles in the process of assembly (57) are found in association with the newly formed membranous structures.

Electron micrographs consistent with the budding of the poliovirus-induced membranes from the endoplasmic reticulum (ER) have been obtained (7). The membranes of the protein secretory pathway are logical candidates for the origin of the poliovirus-induced membranous structures because of the observation that brefeldin A, which inhibits protein secretion, also inhibits poliovirus RNA synthesis (45, 51). Furthermore, structures with the typical morphology of Golgi stacks are not observed (16) and the cellular secretory pathway is inhibited (25) in poliovirus-infected cells.

To determine the intracellular origin of the poliovirus-induced membranes, we have used immunoisolation techniques to isolate membranes that contain the poliovirus replication protein 2C from infected cells. These preparations were tested with antibodies to proteins from throughout the cellular secretory pathway. We found that the 2C-containing membranes did not contain markers from a single donor organelle; instead, markers from throughout the secretory pathway, including the rough ER (rER), the Golgi apparatus, and lysosomes were found in the poliovirus-induced membranes. The presence of viral proteins as well as markers from the late Golgi apparatus and lysosomes was confirmed by electron microscopy and immunocytochemistry of poliovirus-infected cells preserved by high-pressure freezing. These micrographs also revealed that the membranous structures are bounded by two lipid bilayers, not the single bilayer predicted by a simple budding mechanism. The double membranes and the complex biochemical origin of the poliovirus-induced structures instead suggest that they originate by a process analogous to the formation of autophagic vacuoles.

* Corresponding author. Present address: Department of Microbiology and Immunology, Stanford University School of Medicine, Stanford, CA 94305. Phone: (415) 498-7075. Fax: (415) 498-7147. Electronic mail address: karlak@leland.stanford.edu.

† Present address: ZLB Zentrallaboratorium, Blutspendedienst SRK, Wankdorfstrasse 10, CH-3000 Bern 22, Switzerland.

MATERIALS AND METHODS

Cells and virus. HeLa cells grown in suspension and COS-1 cells grown on plates were infected with poliovirus as described previously (25, 51). Infections with poliovirus type 1 Mahoney were performed at multiplicities of infection of 20 to 30 PFU per cell.

Antibodies. The monoclonal antibody against the nonstructural poliovirus protein 2C has been described elsewhere (7, 8, 10, 54). A monoclonal antibody against poliovirus protein 3D was prepared by Kurt Christiansen (University of Colorado Health Sciences Center), using purified recombinant 3D (55) as the immunizing antigen. Rabbit polyclonal antiserum against protein disulfide isomerase (PDI) was provided by Steven Fuller (European Molecular Biology Laboratory, Heidelberg, Germany). A monoclonal antibody (G1/296) against the ER membrane protein p63 (63) was provided by Hans-Peter Hauri (University of Basel, Basel, Switzerland). Although p63 was originally thought to be a marker for the intermediate compartment, p63 localization was reassessed in a recent study and shown to be the rER (64). Polyclonal antibodies against human 1,4-galactosyltransferase (galT) (74) were provided by Eric Berger (Universität Zürich, Zürich, Switzerland). Polyclonal rabbit antibodies against the human lysosomal membrane glycoprotein lamp-1 (15) were provided by Minoru Fukuda (Cancer Research Center, La Jolla, Calif.).

Subcellular fractionation of radiolabeled infected cells. Poliovirus-infected COS-1 cells were labeled from 4 to 4.5 h postinfection (hpi) with [^{35}S]methionine and chased with unlabeled methionine for 15 min as described previously (25). A cytoplasmic extract was prepared as described previously (14) except that cell lysis was performed in the presence of the protease inhibitors phenylmethylsulfonyl fluoride (174 μg/ml), pepstatin (0.7 μg/ml), aprotinin (2 μg/ml), and leupeptin (0.5 μg/ml). After cell disruption in lysis buffer (10 mM Tris [pH 8.0], 10 mM NaCl, 1 mM $MgCl_2$), additional NaCl was added from a 4.0 M stock to a final concentration of 160 mM. The cytoplasmic extracts were layered onto discontinuous sucrose gradients composed of 45, 30, and 10% sucrose in Tris-buffered saline (TBS; 160 mM NaCl, 1.5 mM $MgCl_2$, 10 mM Tris [pH 7.4]). Membranes were spun to equilibrium (14) in an SW41 rotor. Fractions were collected manually from the top of each gradient. Before resolution by sodium dodecyl sulfate-polyacrylamide gel electrophoresis (SDS-PAGE) and autoradiography, proteins were precipitated with trichloroacetic acid as described previously (11).

Immunoisolation of poliovirus-induced membranes. Infected HeLa cells were harvested 5.5 hpi, and cytoplasmic extracts were prepared as described above. Preparations from infected and uninfected cells were adjusted to the same optical density at 600 nm by the addition of lysis buffer; optical densities at 600 nm were typically 0.7 to 1.1. The extracts were adjusted to final concentrations of 160 mM NaCl and 5 mg of bovine serum albumin (BSA) per ml. To 1 ml of these suspensions, 375 μl of anti-2C monoclonal antibody was added. The solutions were incubated overnight at 4°C with constant rotation and then loaded onto discontinuous sucrose gradients. The membranes were spun to equilibrium in an SW50 rotor (14). Fractions of interest were diluted with TBS to a final sucrose concentration of 18% (wt/vol), supplemented with BSA to a final concentration of 5 mg/ml, and incubated with 1 mg of sheep anti-mouse immunoglobulin-coupled magnetic beads (Dynabeads M450; Dynal, Inc., Great Neck, N.Y.) per ml at 4°C for 2 h with constant rotation. Beads were collected by using a magnetic rack (Dynal) and washed twice with TBS containing 5 mg of BSA per ml and twice with TBS. In most experiments, the washed membranes were resuspended in a small volume of TBS containing 1% Triton X-100 and phenylmethylsulfonyl fluoride (174 μg/ml) for 30 min on ice. The supernatant containing the detergent-soluble material was then removed, and the pellet containing the beads and antibody-bound material was washed three times with TBS containing 1% Triton X-100.

Electron microscopy of magnetic beads, SDS-PAGE, and quantitative immunoblotting. Magnetic beads with and without bound constituents were fixed and prepared for electron microscopy as described previously (31). Proteins were separated by SDS-PAGE (48). Gels were stained with silver as reported previously (12) or electroblotted onto Immobilon-P membranes (Millipore, Bedford, Mass.) as described previously (70). Blots were tested sequentially with different primary antibodies followed by horseradish peroxidase-conjugated anti-rabbit or anti-mouse secondary antibodies, using enhanced chemiluminescence as instructed by the manufacturer (Amersham, Arlington Heights, Ill.). Relative protein abundances in immunoisolated membrane preparations were determined densitometrically as described recently (36, 42). Standard curves for each protein analyzed were created from a dilution series of the unfractionated cytoplasmic extract. Briefly, the density of the Western blot (immunoblot) signal for a particular protein immunoisolated with poliovirus-induced membranes was measured. On the same blot, the densities of the same protein were measured from a dilution series of total cytoplasmic extract. The amount of the particular protein in the immunoisolated material was then expressed as a fraction of the volume of cytoplasmic extract in which an equivalent amount of the protein was found. This value was then normalized to a similar value for 3D polymerase. The resulting value should then represent the relative consumption of the compartment in formation of the virus-induced membranes.

High-pressure freezing and freeze-substitution. For cryofixation and electron microscopy, HeLa cells were infected in spinner culture as described previously (51). At 4 to 5 hpi, the cells were washed once in Dulbecco's modified Eagle's medium, resuspended in Dulbecco's modified Eagle's medium containing 0.15 M sucrose, and kept at room temperature (15 to 45 min) until further processing. Samples were centrifuged at room temperature for 3 min at 240 × *g*. Cell pellets were gently vortexed in a minimal volume of the supernatant to create a thick slurry of cells. Aliquots of the slurry were frozen in a Balzers HPM 010 high-pressure freezing apparatus as described previously (20) and stored in liquid nitrogen. Three separate freeze-substitution protocols were used. For observation of cellular morphology, samples were freeze-substituted in 2% osmium tetroxide in acetone at −80°C, gradually warmed to room temperature, en bloc stained in 0.5% uranyl acetate in acetone, and embedded in Epon-Araldite resin. To enhance membrane staining, some samples were freeze-substituted in 0.1% tannic acid (24) in acetone at −80°C, rinsed in acetone, then warmed to −20°C in the presence of 2% osmium tetroxide in acetone for 16 h, and incubated at 4°C for 4 h. After being rinsed in acetone at 4°C, these samples were also embedded in Epon-Araldite resin. For immunolabeling, frozen samples were freeze-substituted in 0.01% osmium tetroxide in acetone at −80°C, warmed to −20°C for 3 h, rinsed in acetone, then en bloc stained with 0.5% uranyl acetate at −20°C for 2 h, embedded at −20°C in Lowicryl K4M, and subjected to polymerization under UV light at −35°C. Thin sections were stained with 2% uranyl acetate and lead citrate and then imaged at 80 kV in a JEOL 100C or Philips CM10 electron microscope.

Immunogold labeling of high-pressure-frozen cells. Thin sections of high-pressure-frozen, freeze-substituted cells embedded in Lowicryl were mounted on Formvar-coated nickel grids and immunolabeled as follows. Grids were floated on a drop of blocking solution in phosphate-buffered saline (PBS) containing concentrations of BSA, Tween 20, fish gelatin (Janssen Life Sciences), and NaCl that corresponded to the concentrations used for each primary antibody. The anti-2C antibody was diluted twofold in PBS that contained 1% BSA and 0.1% Tween 20. The anti-3D antibody was diluted twofold in PBS that contained 1% BSA, 0.1% Tween 20, 0.1% fish gelatin, and an additional 100 mM NaCl. Anti-galT antibodies were diluted 50-fold in PBS that contained 1% BSA, 1% Tween 20, 0.1% fish gelatin, and an additional 100 mM NaCl. Anti-lamp-1 antibodies were diluted 10-fold in PBS that contained 1% BSA, 0.5% Tween 20, and 0.1% fish gelatin. Grids were incubated with primary antibodies for 2 h at room temperature. Gold-coupled secondary antibodies and protein A-gold (Ted Pella Inc., Redding, Calif.) were diluted 10-fold in PBS that contained 1% BSA and 0.1% Tween 20 and incubated with the grids for 1 h at room temperature.

In single-labeling experiments, mouse monoclonal primary antibodies were detected with goat anti-mouse secondary antibodies coupled to 15-nm-diameter gold particles. Polyclonal rabbit antibodies were challenged with protein A–15-nm gold particle complexes.

For double labeling, the sections were incubated with the primary antibody followed by an incubation with goat anti-rabbit or goat anti-mouse secondary antibodies coupled to 15-nm gold particles. The grids were then incubated with the second antibody followed by goat anti-mouse or goat anti-rabbit secondary antibodies coupled to 5-nm gold. In all double-labeling experiments, the first and second primary antibodies were from different animal species.

RESULTS

Immunoisolation of poliovirus-induced membranes. Several protocols for isolating poliovirus-induced membranes have used fractionation of cytoplasmic extracts in discontinuous sucrose gradients (9, 10, 14, 69). Poliovirus proteins 2C, 3AB, 3CD, and 3D and viral capsid precursors all copurify with poliovirus-induced membranes in such gradients (8, 9, 14, 57, 67–69, 71). In gradients containing layers of 30 and 45% sucrose, the comigration of poliovirus protein 2C with membranes that collected on top of the 30 and 45% sucrose layers has been demonstrated (8, 10). RNA-dependent RNA polymerase activity from endogenous templates was demonstrated in both fractions (8), making these fractions good candidates to contain most components of the active poliovirus RNA replication complexes and the membranes associated with them in the infected cell.

To determine where viral proteins sedimented in gradients composed of 45, 30, and 10% sucrose, poliovirus-infected COS-1 cells were labeled with [^{35}S]methionine from 4.5 to 5 hpi prior to fractionation. Polioviral protein 2C, known to be present in viral replication complexes, was found predominantly in the pellet and on top of the 45% sucrose fraction (m_2), in agreement with results of the original study using this isolation protocol (69). Since the m_2 fraction is known to display RNA-dependent RNA polymerase activity (8), we initially

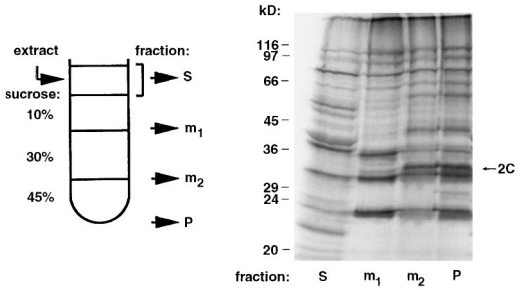

FIG. 1. Fractionation of poliovirus-infected COS-1 cell extracts. Infected cells were labeled with [^{35}S]methionine from 4 to 4.5 hpi with poliovirus and subjected to subcellular fractionation on sucrose gradients as indicated. Proteins were precipitated, separated by SDS-PAGE, and visualized by autoradiography. The migration of protein markers and the migration of membrane-associated poliovirus protein 2C are indicated. Similar patterns were obtained from infected HeLa cells. S, supernatant; P, pellet.

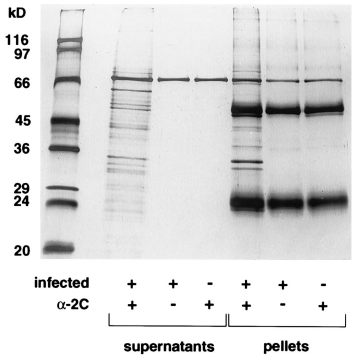

FIG. 3. Total proteins immunoisolated from the m_2 fraction of infected HeLa cells. Total proteins from immunoisolations and mock immunoisolations were separated into those that dissociated from viral protein 2C in the presence of Triton X-100 detergent (supernatants) and those that remained associated (pellets). Proteins were separated by SDS-PAGE and visualized by silver staining. Migration of marker proteins is shown on the left. The 66-kDa protein present in all lanes is BSA, which was used as a blocking agent. Antibody polypeptides of 50 and 25 kDa are visible among the bead-bound proteins. Viral protein 2C migrates with an apparent molecular mass of 34 kDa and can be seen in the infected, α-2C (anti-2C antibody) pellet fraction.

chose the m_2 fraction as a source of membranes for further biochemical purification.

Immunoisolation with antibody-coupled magnetic beads was used to isolate only those membranes that were directly associated with the viral replication complex. HeLa cells grown in spinner culture were used to make the growth of large quantities of cells more practical. Viral protein 2C was chosen as a target for immunoisolation because its peripheral association with the cytoplasmic face of intracellular membranes (8, 10) is very stable, resisting extraction with 2 M urea (69). Using a monoclonal antibody against protein 2C (54), we first tested whether immunoisolation was specific for 2C-containing membranes. Extracts from infected HeLa cells were prepared and incubated with the anti-2C monoclonal antibody. The membranes were centrifuged to equilibrium in discontinuous sucrose gradients as diagramed in Fig. 1, separating the membranes into m_1, m_2, and pellet fractions and leaving unbound antibody in the supernatant. Antibody-bound material from the m_2 fraction was then isolated by using magnetic beads coupled to sheep anti-mouse antibody. Controls for these immunoisolations included performing the same isolation procedure with extracts from uninfected HeLa cell extracts and performing the isolation with infected HeLa cells in the absence of the anti-2C antibody.

The magnetic beads were analyzed by electron microscopy following chemical fixation (Fig. 2). Membranous material was successfully isolated only when the anti-2C antibody was incubated with extracts from infected cells. The protein content of the immunoisolated material was examined by SDS-PAGE (Fig. 3). Again, it is clear that proteins were immunoisolated from infected extracts, but not from uninfected extracts, and only in the presence of primary antibody to poliovirus protein 2C. Some of the immunoisolated proteins were released in the presence of the detergent Triton X-100 (Fig. 3, supernatants), indicating that they were associated primarily with the membranes and not with stable 2C-containing protein complexes. It is in these fractions that all of the cellular markers described here (PDI, p63, galT, and lamp-1) were found. However, many proteins remained bound to the antibody-complexed magnetic

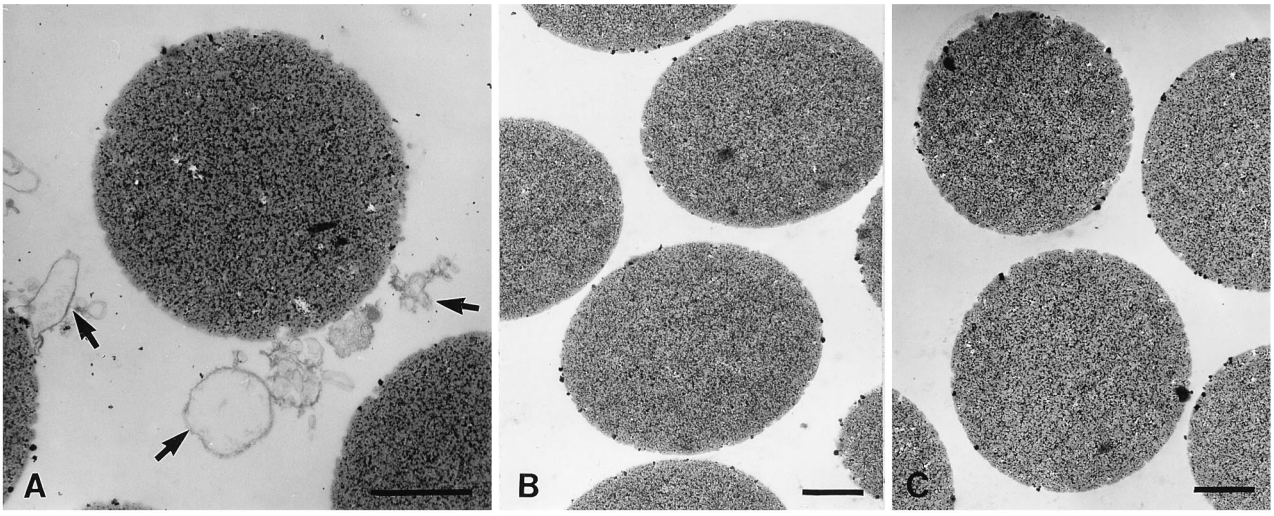

FIG. 2. Immunoisolation of poliovirus-induced membranes from the m_2 fraction of infected HeLa cells. Cell extracts were incubated with an anti-2C monoclonal antibody, and membranes from the m_2 fraction were adsorbed to magnetic beads coupled to sheep anti-mouse antibodies. Membrane isolations from infected (A and B) and uninfected cells (C) were performed in the presence (A and C) and absence (B) of anti-2C antibody. Arrows indicate isolated membranes. Bars indicate 1 μm.

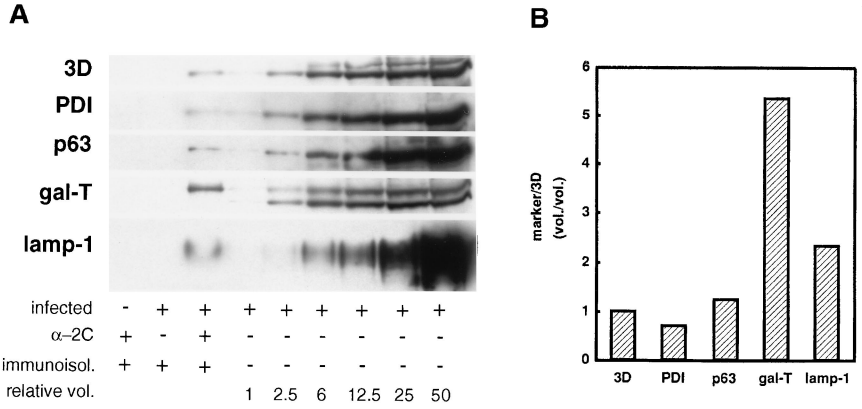

FIG. 4. Determination of relative amounts of cellular proteins in m_2 fractions by quantitative immunoblotting. 2C-containing material was immunoisolated from m_2 fractions of infected HeLa cells. Proteins removed from the beads by incubation with Triton X-100 were separated by SDS-PAGE and transferred to Immobilon-P membranes. (A) The same blot was tested for the presence of the poliovirus RNA-dependent RNA polymerase 3D and the cellular proteins indicated on the left. The relative representation of each protein in the immunoisolated material was determined densitometrically. A standard curve for each protein was created from a dilution series of unfractionated cytoplasmic extract. (B) The representation of each protein in the immunoisolated material from infected cells was normalized to the representation of 3D. α-2C, anti-2C antibody.

beads even in the presence of detergent (Fig. 3, pellets). Although sufficient Western analysis has not been performed to identify the proteins in this fraction unambiguously, this fraction probably includes viral proteins of the poliovirus replication complex (10, 13, 56, 67) and possibly cellular proteins that interact directly or indirectly with the viral replication complex (4, 40, 52).

Immunoisolated poliovirus-induced membranes contain markers from several compartments of the protein secretory apparatus. The immunoisolated membranes were tested for the presence of viral and cellular proteins by immunoblotting. We tested for the presence of several organelle-specific cellular proteins to determine the cellular origin of the virus-induced membranes. The amount of each viral and cellular protein relative to its abundance in the unfractionated cytoplasmic extract was determined.

The viral protein tested was $3D^{pol}$, the RNA-dependent RNA polymerase and clearly a key enzyme of the viral replication complex. Cellular proteins chosen are known to localize to different cellular compartments along the protein secretory pathway: PDI, a peripheral membrane protein present in the lumen of the ER (37, 47); p63, a 63-kDa integral ER membrane protein (64); galT, an enzyme found in both the *trans*-Golgi network (TGN) and the *trans* cisternae of the Golgi apparatus (59); and lamp-1, a lysosomal membrane glycoprotein (15).

The representation of the various marker proteins was determined by densitometry and normalization to that of immunoisolated 3D (Fig. 4; Materials and Methods). All cellular markers tested were present in the immunoisolated membranes but not in control isolations prepared in the absence of anti-2C antibody or from uninfected cells (Fig. 4A). Marker proteins from different compartments of the secretory apparatus, however, were present in different relative abundances in the m_2 fraction (Fig. 4B). For example, a sevenfold-higher representation of galT than of PDI was found in the immunoisolated membranes. The form of galT found in the poliovirus-induced membranes (Fig. 4A) was, interestingly, exclusively the mature form that results from processing in the Golgi apparatus (66). We also found a two-fold-higher representation of the lysosomal marker lamp-1 than of the ER marker in the immunoisolated membranes. All cellular markers could be extracted by treatment with detergent (data not shown), suggesting that these proteins were associated with the membranes of the poliovirus replication complex and probably not with the replication complex itself.

The localization of these marker proteins with the 2C-containing membranes could indicate that these membranes were actually derived from compartments throughout the secretory apparatus. Alternatively, the immunoisolated material could be contaminated with membranes from organelles that were not constituents of the 2C-containing membranes in the cell. Since control preparations showed negligible amounts of cellular and viral proteins, such contamination could have occurred only during membrane immunoisolation from poliovirus-infected cells. To address the possibility that the poliovirus-induced membranes adhered to marker proteins or membranes from irrelevant organelles during immunoisolation, a mixing experiment was performed. The amount of labeled galT, labeled lamp-1, and total labeled protein in immunoisolated material from a mixture of extracts from infected unlabeled and uninfected labeled cells was approximately 25% of the amount isolated from the labeled infected extract alone (data not shown). Thus, at least 75% of the material shown in Fig. 4 was isolated by virtue of its direct association with 2C-containing membranes in infected cells.

Membranes containing viral protein 2C differ in content of cellular proteins. To test whether the 2C-containing membranes in the cell other than those found in the m_2 fraction also contained PDI, p63, galT, and lamp-1 in the same relative proportions as in the m_2 fraction, different sucrose gradients were used in the recovery of the 2C-containing membranes. To recover 2C-containing membranous material with a higher buoyant density than m_2 (Fig. 1, pellet), gradients composed of 60, 45, and 30% sucrose were used, and the membranes on top of the 60% sucrose were collected as the m_3 fraction (Fig. 5A). To recover most of the vesicular membrane material from infected cells, sucrose gradients composed of 60 and 10% sucrose were used, and a total fraction was collected (Fig. 5B). Again, almost all the proteins recovered from anti-2C immunoisolations were specific for infected cells and the presence of the antibody (Fig. 5).

All cellular markers found in the m_2 fraction (Fig. 4) were also present in the m_3 and total fractions, although with different relative abundances (Fig. 6). Specifically, the m_3 fraction contained higher relative amounts of the ER markers PDI and

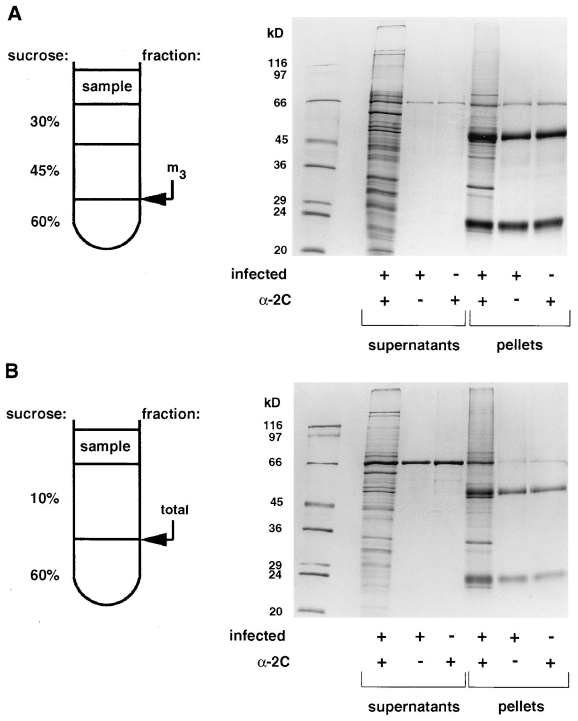

FIG. 5. Immunoisolation of poliovirus-induced membranes from different subcellular fractions. HeLa cell extracts were centrifuged to equilibrium in discontinuous sucrose gradients as indicated. (A) Fraction m_3 was collected from infected and uninfected cells in the presence and absence of anti-2C antibody (α-2C) as indicated. 2C-associated membranes in the m_3 fractions were immunoisolated. Total proteins in the supernatants and pellets obtained after incubation with Triton X-100 are displayed by SDS-PAGE and silver staining. (B) A total fraction which should contain m_1, m_2, and m_3 membranes was collected as indicated. Proteins associated with immunoisolated membranes in detergent-sensitive (supernatants) and detergent-resistant (pellets) manners are displayed.

p63 than the m_2 fraction. The consistently low representation of the ER marker PDI may result from its being the only lumenal marker used in this study. Clearly, the m_2 and m_3 fractions could be physically separated on the basis of their differing buoyant densities. Thus, membranes that contain poliovirus replication proteins are heterogeneous in physical properties and possibly in origin. In the total fraction, which presumably best represents the intracellular situation, membranes from the ER, *trans*-Golgi stack and TGN, and lysosomes were recruited to the 2C-containing membranes in amounts comparable to their representation in total cytoplasmic extracts.

Poliovirus infection results in the accumulation of structures surrounded by two membranes. To examine the poliovirus-induced membranous structures directly, we examined poliovirus-infected and uninfected cells by electron microscopy, using high-pressure freezing and freeze-substitution methods (reviewed in references 20, 33, and 53) instead of chemical fixation to preserve as much membrane fine structure as possible. The advantages of high-pressure freezing and freeze-substitution over chemical fixation are extremely rapid immobilization and fixation of cellular components and improved preservation of labile or transient cellular structures, particularly membranes (20). To our knowledge, this is the first study that has used fixation by high-pressure freezing to analyze the membrane rearrangements in poliovirus-infected cells. Infected HeLa cells were collected 4 to 5 hpi and processed for electron microscopy. A dramatic accumulation of aggregated membranes in the cytoplasm of infected, but not uninfected, cells was observed (Fig. 7A and B), in agreement with previous reports of poliovirus-induced "vesicles" 50 to 500 nm in diameter (8, 10, 16, 21).

Whereas most studies of chemically fixed poliovirus-infected cells have suggested that infection induces the formation of vesicles bounded by a single membrane, the vesicles observed in infected cells preserved by high-pressure freezing were bounded by a cisterna-like structure with an electron-lucent lumen of fairly uniform width (Fig. 7). Inclusion of tannic acid in the freeze-substitution protocol resulted in sufficient electron-dense staining of the virus-induced membranes to visualize the two limiting bilayers (Fig. 8A). This cisterna-like structure surrounded a darker center of apparently variable composition that was sometimes similar in appearance to the cytoplasm but sometimes exhibited a more fibrous morphology. Viral capsids were frequently observed within the enclosures, but the vast majority of viral particles were found in the cytoplasm adjacent to clusters of the virally induced membrane structures (Fig. 7C).

Further support for the presence of two lipid bilayers in the poliovirus-induced membranous structures comes from the horseshoe configuration of many of them (Fig. 8B). These images are suggestive of membrane-limited cisterna in the process of enclosing a region of cytoplasm, before closure of the compartment is complete.

Even at early times postinfection, all membranous structures that have formed as a result of poliovirus infection appear to be limited by the cisterna-like structure. Figure 8C shows a portion of an infected cell 2.5 hpi in which the membranes of both the ER and the virally induced vesicular structures are unstained but the greater thickness of the latter suggests the presence of a double membrane. Therefore, double-membrane structures represent the morphology of the virally induced membranes throughout poliovirus infection and are not the result of events that occur only as the cells near lysis.

Poliovirus, TGN, and lysosomal proteins are localized to double-membrane structures in poliovirus-infected cells. To confirm that the double-membrane structures correspond to the poliovirus-induced membranes, we tested the intracellular localization of poliovirus proteins 2C and 3D polymerase by immunostaining the cryofixed samples. In agreement with previous reports (7, 54, 72), we found that 2C epitopes localized almost completely to the area of the rearranged membranes, with most of the labeling associated with the outer surface of the double-membrane structure (Fig. 9A). The same membrane association was found for 3D polymerase-containing polypeptides (Fig. 9B). These findings corresponded to earlier biochemical (13, 69) and morphological (72) studies, all of which localized $3D^{pol}$ and its precursors to the rearranged intracellular membranes. Therefore, the double-membrane structures that we observed correspond to the membranous vesicles previously described.

To test the presence of proteins from the cellular secretory pathway in the rearranged double-membrane structures, the localizations of galT from the *trans*-Golgi and the TGN (Fig. 9C) and lamp-1 from lysosomes (Fig. 9D) were analyzed. Antibodies available to the ER markers did not stain well following cryopreservation in either infected or uninfected cells. Many more gold particles corresponding to galT and lamp-1 were found in the virus-induced double-membrane structures (Fig. 9C and D) than in cytoplasm that did not contain these membranes (data not shown; see Fig. 10). Neither galT nor lamp-1, however, localized completely to the rearranged membranes. In particular, lamp-1 was often found in larger mem-

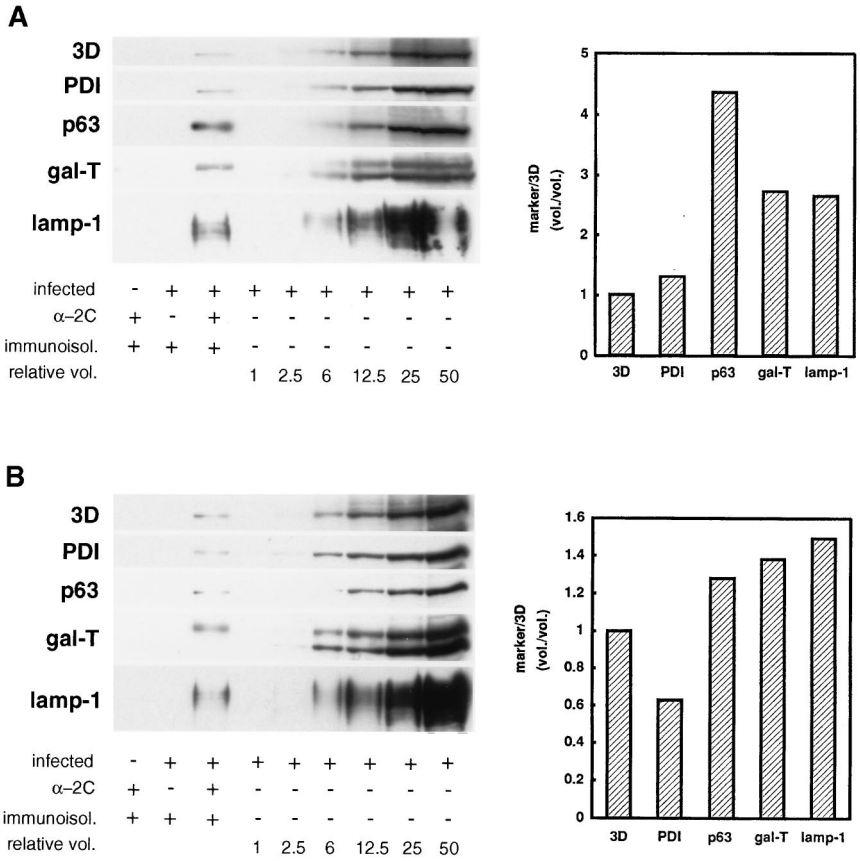

FIG. 6. Quantitative immunoblots to determine relative amounts of cellular proteins immunoisolated from m_3 (A) and total (B) fractions. Proteins were dissociated from the magnetic beads with detergent, 2C-containing material was isolated, and the relative representation of each cellular marker in the immunoisolated material was determined as described for Fig. 4. α-2C, anti-2C antibody.

branous structures close to the smaller membranous structures (Fig. 9D).

Colocalization of *trans*-Golgi and lysosomal proteins in 2C-containing double-membrane structures. Immunoisolation of membranes that contained PDI, p63, galT, and lamp-1 with antibody against poliovirus protein 2C (Fig. 4 and 6) argued that the poliovirus-induced membranes, or at least membranes that contain poliovirus proteins, are derived from membranes from throughout the protein secretory apparatus. To confirm further that the double-membrane structures that contain poliovirus proteins and those that contain cellular markers are the same structures, colocalization of poliovirus protein 2C and galT and lamp-1 was performed. These double-labeling experiments demonstrated the colocalization of galT and poliovirus 2C (Fig. 10A) and of lamp-1 and 2C (Fig. 10B) in the double-membrane structures that accumulate during poliovirus infection. Furthermore, galT and lamp-1 both selectively labeled the electron-lucent membranes, not the darker regions enclosed by the double membranes, arguing that *trans*-Golgi and lysosomal membranes contributed directly to the double-membrane structures and were not simply contained within the membrane-bounded region as cytoplasmic constituents.

DISCUSSION

Poliovirus-induced membranes contain markers from throughout the protein secretory pathway. Biochemical isolation of poliovirus-induced membranes was performed by immunoisolation of membranes that were physically associated with viral protein 2C in infected cells. This material was shown to be specific to viral infection by the absence of isolated material in the absence of the anti-2C antibody or when the immunoisolations were performed from lysates of uninfected cells.

PDI and p63, proteins normally found in the ER, were present in these virus-specific membranes, but proteins from later in the secretory pathway, from the Golgi apparatus and from lysosomes, were equivalently represented (Fig. 4 and 6). This is surprising, considering that images consistent with the direct formation of the poliovirus-induced membranes from the rER have been obtained frequently (7). Furthermore, the inhibition of poliovirus RNA replication by brefeldin A (45, 51), which inhibits ER-to-Golgi traffic, made the ER seem a likely source for the origin of these membranes (51). ER membranes are the most abundant intracellular membranes (38). From our biochemical results, we conclude that the ER constitutes a significant but not exclusive source for the poliovirus-induced membranous structures.

An integral membrane protein from the *trans*-Golgi stack and TGN, galT, was highly represented in the m_2 fraction. Immunostaining of membranes visualized by electron microscopy demonstrated the presence of galT in the double-membrane structures (Fig. 9C) and confirmed its colocalization with poliovirus protein 2C (Fig. 10A). Only the more mature form of galT was observed in the immunoisolates (Fig. 4A and 6A). Although poliovirus infection is known to cause a marked

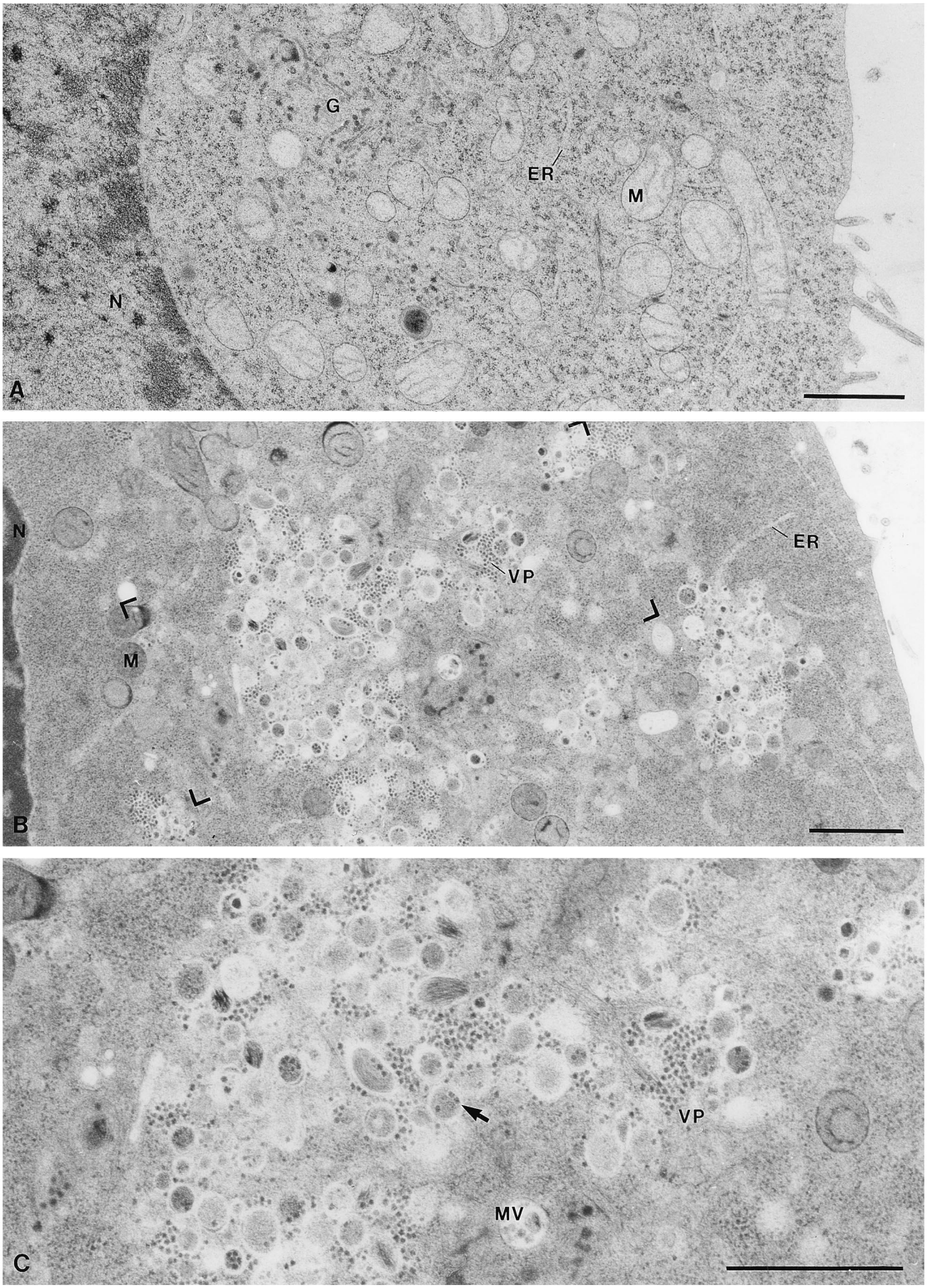
G
ER
M
N
A
N
VP
ER
M
B
VP
MV
C

FIG. 7. Morphology of poliovirus-induced membranes in HeLa cells preserved by high-pressure freezing. (A) Uninfected HeLa cell; (B) poliovirus-infected HeLa cell 5 hpi; (C) bracketed region of panel B at higher magnification. N, nucleus; G, Golgi cisternae; ER, rER; M, mitochondrion; VP, viral particles. Multivesicular bodies (MVs) were morphologically distinguishable from the poliovirus-induced membranous structures and were far less numerous. Arrow indicates a poliovirus-induced structure with viral particles in the enclosed region. Freeze-substitution was with osmium and uranyl acetate. Bars indicate 1 μm.

decrease in the rate of exocytic transport as measured by pulse-chase experiments, galT that displays Golgi apparatus-specific modifications is still present in the total intracellular pool which can be sampled by Western analysis. The presence of *trans*-Golgi stack-specific forms of galT in the double-membrane structures induced by poliovirus infection argues that these forms were derived at least in part from the *trans*-Golgi stack or the TGN itself and not exclusively from membranes that contained galT en route to its destination. A relatively high proportion of Golgi apparatus-derived membranes in the poliovirus-induced membrane fraction provides an explanation for the observation that clearly recognizable Golgi stacks are absent from poliovirus-infected cells (16).

Lamp-1, an integral membrane protein found in mature lysosomes, was also highly represented in the poliovirus-induced membranes. Immunostaining of electron microscopy

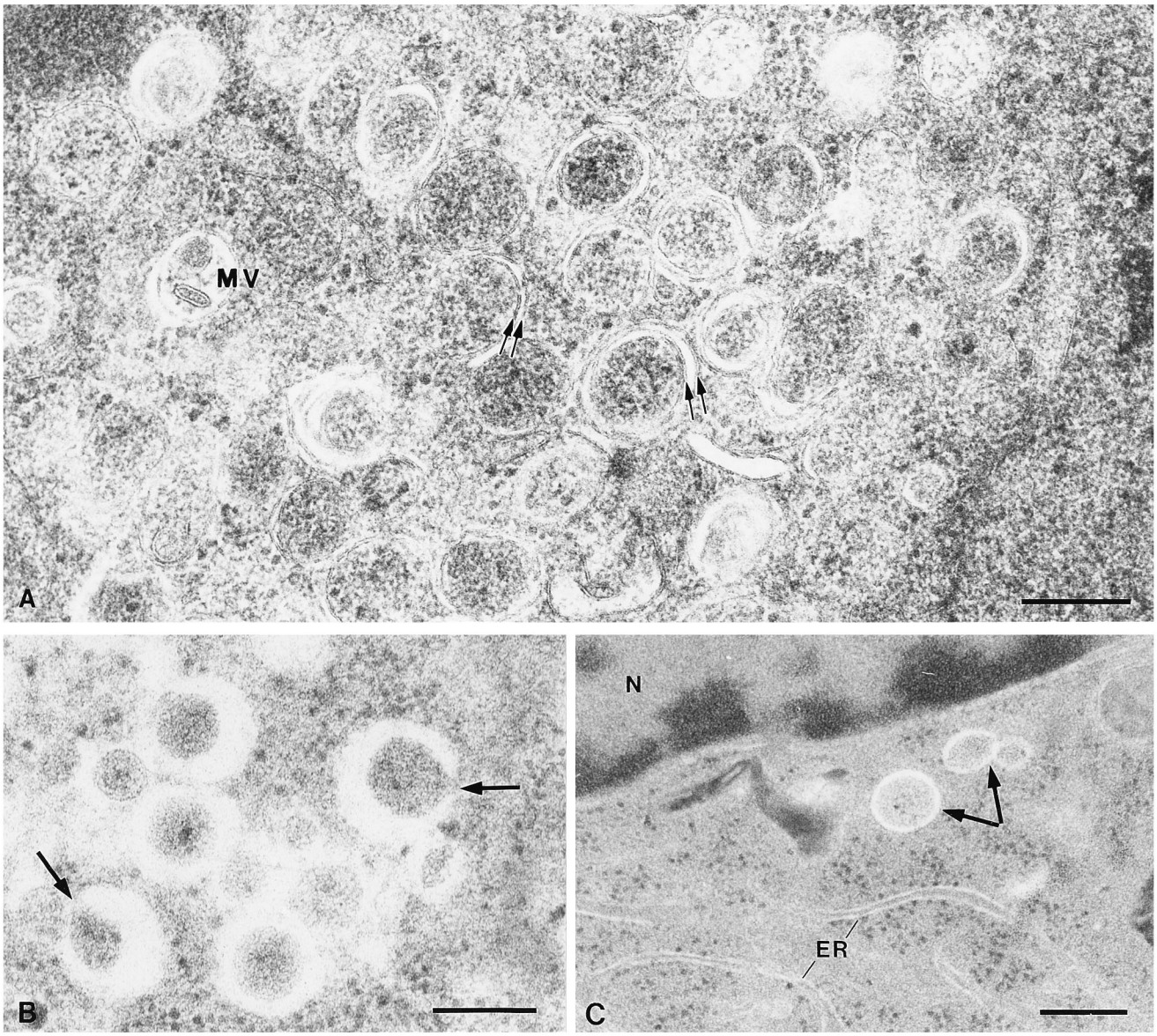

FIG. 8. Detailed morphology of poliovirus-induced membranes preserved by high-pressure freezing. (A) HeLa cell 5 h after infection with poliovirus at higher magnification. Paired arrows, examples of two adjacent phospholipid bilayers; MV, multivesiculate body characteristic of structures also found in uninfected cells. Grids were stained sequentially with lead citrate, 2% uranyl acetate, and lead citrate. (B) Selected horseshoe-shaped membranes 5 hpi. Arrows indicate the opening between the enclosed region and the cytoplasm. (C) A poliovirus-infected HeLa cell 2.5 hpi. Arrows indicate structures identical with poliovirus-induced membranes observed at later times postinfection. Membranes whose distribution and morphology are characteristic of ER are marked. N, nucleus. Bars indicate 0.2 μm.

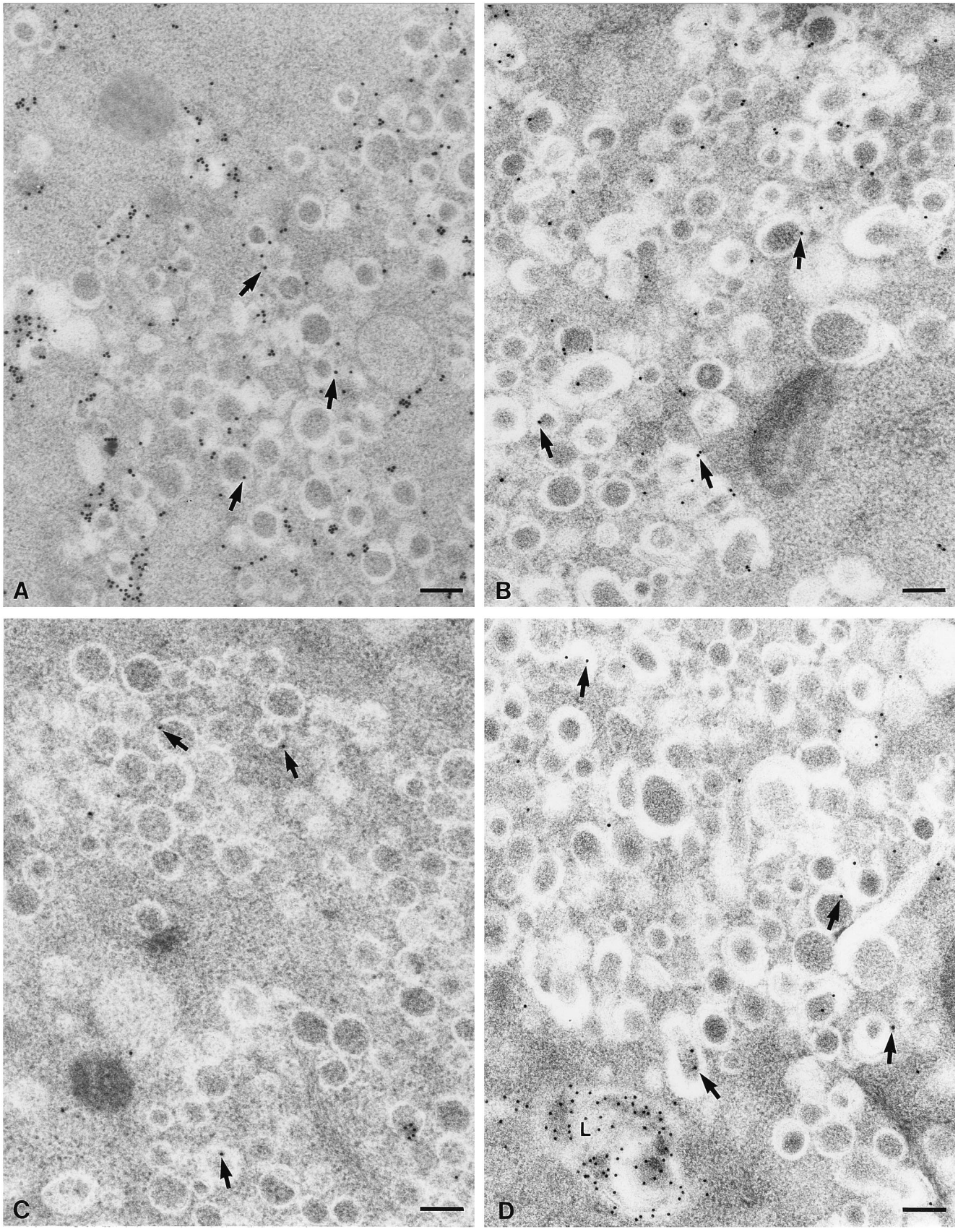

FIG. 9. Localization of polioviral and cellular proteins to poliovirus-induced membranes. Sections of infected HeLa cells were labeled with 15-nm gold particles coupled to secondary antibodies; arrows indicate selected gold particles. Primary antibodies recognized poliovirus proteins 2C (A) and 3D (B) and cellular proteins galT (C) and lamp-1 (D). Low-temperature embedding was in Lowicryl. L, lysosome. Bars indicate 0.2 μm.

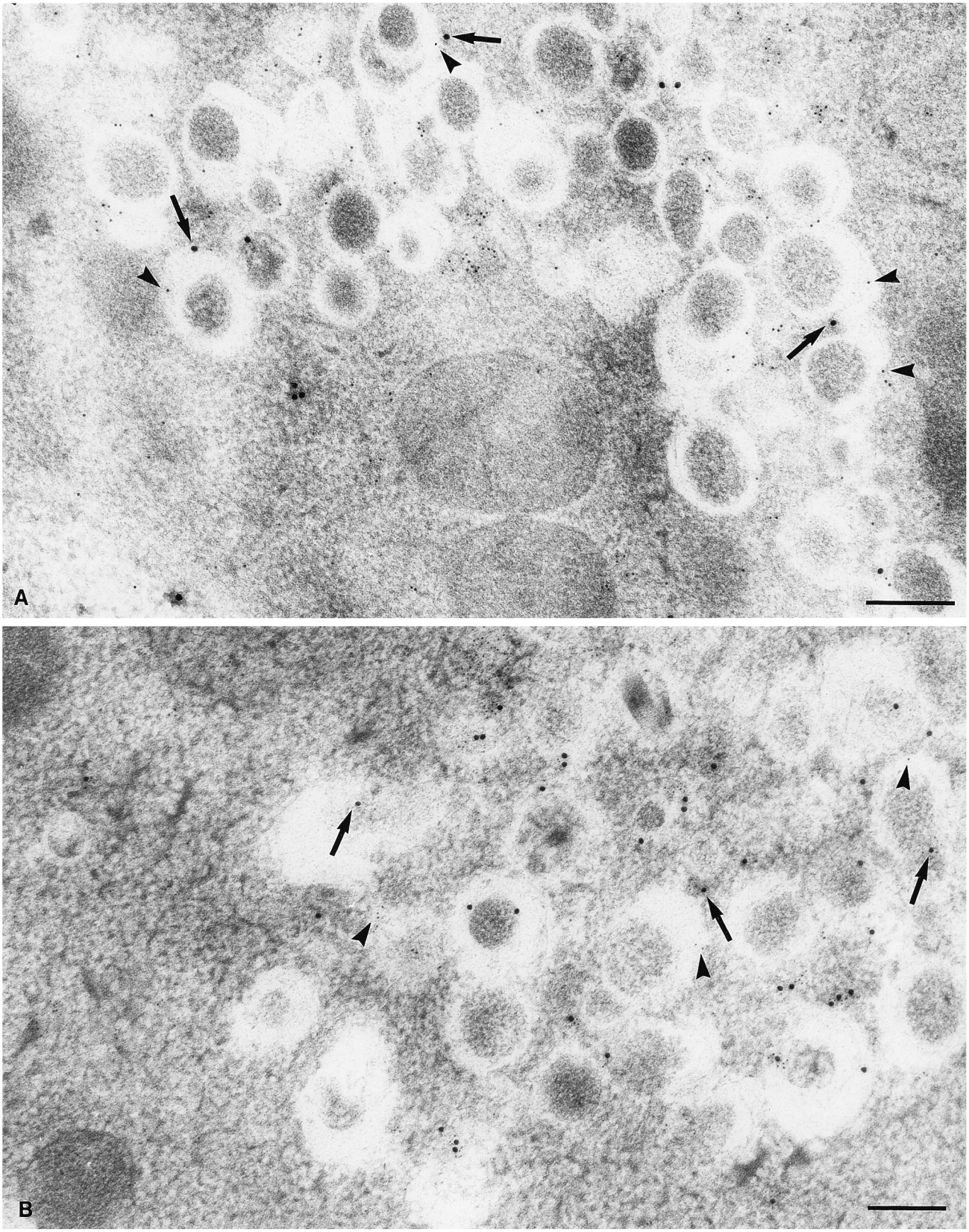

FIG. 10. Colocalization of polioviral and cellular proteins to virus-induced membranes. Sections of infected HeLa cells preserved by high-pressure freezing were labeled for galT with 15-nm gold particles (arrows) and viral protein 2C with 5-nm gold particles (arrowheads) (A) and for 2C with 15-nm gold particles (arrows) and lamp-1 with 5-nm gold particles (arrowheads) (B). Bars indicate 0.2 μm.

sections confirmed instances of its localization to membranes that also contained poliovirus protein 2C (Fig. 9B). However, most of the lamp-1-specific staining was found in larger membranous structures (Fig. 8D and 9B), which may represent bona fide lysosomes. The presence of lysosome-derived constitutents in poliovirus-induced membranes is consistent with the previously observed cytochemical localization of the lysosomal marker acid phosphatase to poliovirus-induced membranes at later stages of infection (41).

The 2C-containing membranes were found to contain proteins normally localized throughout the protein secretory pathway. This could result from any of three different possibilities. First, viral protein 2C could associate nonspecifically with many membranes in the cell, only a subset of which are used to assemble viral RNA replication complexes. However, 2C was found to colocalize with Golgi marker galT, and with lysosomal marker lamp-1, to membranous structures morphologically indistinguishable from the other poliovirus-induced membranes. Therefore, galT- and lamp-1-containing membranes are morphologically representative of the population of poliovirus-induced membranes, and there is no reason to suspect that a subset of these membranes does not contain functional RNA replication complexes. A second possibility for the presence of so many cellular markers in the 2C-containing membranes is that intracellular membranes fuse early in poliovirus infection, and the poliovirus-induced vesicular structures form from a pooled compartment. However, the observation that 2C-containing membranes could be physically separated on the basis of buoyant density into m_2 and m_3 fractions that displayed different relative abundances of cellular markers suggests that these membranes are not derived from a homogeneous pooled compartment. A third possibility, that the poliovirus-induced membranes are formed from several different compartments in the cell, is also consistent with the data presented here.

Poliovirus-induced membranous structures are bounded by double lipid bilayers. To visualize the poliovirus-induced membranes, cryofixation and electron microscopy were used. Over the past 30 years, several electron microscopic studies have described the morphological events associated with poliovirus infection. All of these studies have used chemical fixation, which immobilizes cellular structures in seconds to minutes, forms only selective cross-links, and induces osmotic changes in the membrane-bounded compartments during changes in fixation and washing buffers (33). These problems can be largely overcome by the use of cryofixation methods, which are more rapid (milliseconds) and can immobilize all molecules simultaneously (20, 33). The use of cryofixation methods in the study has provided strong evidence for the formation of double-membrane-bounded structures during poliovirus infection.

Interestingly, double membranes in poliovirus-induced cytoplasmic structures have been observed previously. In 1965, Dales and coworkers used a chemical fixation procedure in which infected cells were exposed briefly to glutaraldehyde before being fixed in osmium and observed poliovirus-induced "membrane-enclosed bodies" which resembled networks of vacuoles with double membranes wrapped around portions of cytoplasm (21). They also observed that the membranes did not always completely enclose the central material. Their hypothesis was that poliovirus-induced membranes resembled "autolytic vacuoles" (21). Autophagic vacuoles, as they are currently termed, are delineated by double membranes and are thought to form by the enwrapping of cytoplasm by membranes derived from the rER (reviewed in reference 29). They contain rER transmembrane proteins in their inner and outer membranes; at later stages of their maturation, the compartment closes by fusion of the two enwrapping double membranes. At this point, lgp120, a lysosomal membrane protein, is acquired in the outer membrane (27, 28).

Mechanism of formation of double-membrane structures. Discussion of the intracellular origin or mechanism of formation of the poliovirus-induced membranes must account for the formation of double membranes. For example, a hypothesis from this laboratory that the poliovirus-induced membranes could be subverted transport vesicles (51) cannot be literally correct, since normal transport vesicles are thought to be formed by simple budding from the organelle of origin (reviewed in reference 60) and should thus be bounded by single membranes.

Double membranes could be acquired by two budding events, in which one vesicle first formed by budding into the ER, Golgi apparatus, or other organelle. The single-membrane vesicle could then bud out of the organelle into the cytoplasm, thus acquiring a second membrane. Alternatively, two membranes could envelope cytoplasm as a result of wrapping, originally forming a horseshoe-shaped structure that could later be sealed. Our observation of some such horseshoe-shaped structures (Fig. 8B and 9C) is more consistent with the latter hypothesis.

As anticipated by Dales et al. (21), precedent for wrapping of cytoplasm exists in the formation of autophagic vacuoles, which can form as a result of amino acid or serum starvation or other cellular stress (reviewed in reference 29). Such vacuoles are thought to form by the wrapping of ER membranes around cytoplasm and cytoplasmic constituents; the resulting horseshoe-shaped structures and the double-membrane spherical vacuoles that they become are termed immature autophagic vacuoles (AV_is). The AV_is mature into degradative autophagic vacuoles (AV_ds) by acquiring degradative enzymes from either mature lysosomes (49) or the prelysosomal compartment (58). Mature AV_ds contain only one membrane; the inner membrane is degraded. However, intermediates in autophagic vacuole maturation ($AV_{i/d}$s) that have acquired certain lysosomal markers, contain two membranes, and have not yet acquired degradative lysosomal enzymes have been identified (28). Maturation of AV_is into AV_ds is inhibited by cycloheximide, an inhibitor of protein synthesis (50). In cells that exhibit autophagy, a partial impairment of protein glycosylation and transport was observed: incompletely glycosylated proteins were delivered directly to lysosomes, bypassing the Golgi apparatus (43, 73). Whether the poliovirus-induced membranous structures represent autophagic vacuoles arrested in their maturation by the viral inhibition of protein synthesis remains to be tested. However, the observation that the virus-induced membranes acquire a lysosomal marker is a further indication that their development parallels that of autophagic vacuoles. Furthermore, the finding of cytoplasmic components, such as poliovirions (Fig. 7C) and mitochondrial inner membrane proteins (data not shown), in the preparations of poliovirus-induced membranes is consistent with the presence of cytoplasm within the enwrapping double membranes.

The poliovirus protein or activity that causes accumulation of the double-membrane structures and rearrangement of the intracellular secretory apparatus has not yet been identified, although there are some likely candidates. Poliovirus protein 2A induces the formation of large electron-dense structures in the cytoplasm of *Saccharomyces cerevisiae* (6). Poliovirus protein 2C, when expressed in vaccinia virus, causes membrane rearrangements that include the formation of vesicular membranes as well as the juxtaposition and stacking of membranes that appear to be derived from the ER, although this has not been tested by immunostaining (1, 16). Poliovirus protein 2BC

expressed by using vaccinia virus vectors also causes the formation of vesicular membrane structures more similar to those observed in poliovirus-infected cells than those formed in the presence of 2C alone (1, 16). Interestingly, 2BC has recently been reported to induce vesicle formation in *S. cerevisiae* as well (5). The expression of 2B alone in human cells by using vaccinia virus vectors or in yeast cells has been reported to have no effect on intracellular membrane structure (1, 5). However, direct transfection of plasmids encoding either 2B or 3A causes the inhibition of protein traffic between the ER and the Golgi apparatus (25). The expression of 3A alone also causes a normally secreted protein to colocalize with PDI, the ER lumenal protein; both the secreted protein and the ER protein were then found redistributed throughout the cytoplasm (25). Viral protein 3A, when expressed in isolation, was found to localize to intracellular membranes that were thought to be ER or Golgi apparatus derived, although their identity was not determined by immunostaining (23).

The experiments described in this report have revealed that the intracellular membrane rearrangements that accompany poliovirus infection result in the formation of double-membrane structures that contain markers from the ER, the *trans*-Golgi stacks and TGN, and lysosomes. The double-membrane structure implies that the membranes do not form by a simple budding mechanism from a discrete compartment in the cell but instead must form either by a double-budding mechanism or, more likely, by wrapping of cytosol by membranous compartments. How viral RNA replication complexes assemble on these membranes, why poliovirus RNA synthesis is inhibited by brefeldin A, and the mechanism of action of the viral proteins that promote membrane rearrangement remain to be discovered.

ACKNOWLEDGMENTS

We are indebted to Kurt Bienz and Denise Egger for their generous gift of anti-2C monoclonal antibody. We thank L. Andrew Staehelin and Kathryn Howell for their insights into cytoplasmic membrane morphology and Anne McBride and Frank Luca for their roles in the preparation of the anti-3D monoclonal antibody. We are grateful to Peter Sarnow, Kurt Bienz, John R. Doedens, Denise Egger, Anne E. McBride, and L. Andrew Staehelin for helpful comments on the manuscript and to Steven Fuller, Hans-Peter Hauri, Eric Berger, and Minoru Fukuda for the provision of antibodies critical to this research.

A.S. was a postdoctoral research associate, and K.K. was an assistant investigator, of the Howard Hughes Medical Institute. A.S. also acknowledges support of the Swiss National Science Foundation. This work was supported by the Howard Hughes Medical Institute and by NIH grant AI-25166.

REFERENCES

1. **Aldabe, R., and L. Carrasco.** 1995. Induction of membrane proliferation by poliovirus proteins 2C and 2BC. Biochem. Biophys. Res. Commun. **206:**64–76.
2. **Amako, K., and S. Dales.** 1967. Cytopathology of mengovirus infection. I. Relationship between cellular disintegration and virulence. Virology **32:**184–200.
3. **Amako, K., and S. Dales.** 1967. Cytopathology of mengovirus infection. II. Proliferation of membranous cisternae. Virology **32:**201–205.
4. **Andino, R., G. E. Rieckhof, P. L. Achacosco, and D. Baltimore.** 1993. Poliovirus RNA synthesis utilizes an RNP complex formed around the 5′ end of viral RNA. EMBO J. **12:**3587–3598.
5. **Barco, A., and L. Carrasco.** 1995. A human virus protein, poliovirus protein 2BC, induces membrane proliferation and blocks the exocytic pathway in the yeast *Saccharomyces cerevisiae*. EMBO J. **14:**3349–3364.
6. **Barco, A., and L. Carrasco.** 1995. Poliovirus 2Apro expression inhibits growth of yeast cells. FEBS Lett. **371:**4–8.
7. **Bienz, K., D. Egger, and L. Pasamontes.** 1987. Association of polioviral proteins of the P2 genomic region with the viral replication complex and virus-induced membrane synthesis as visualized by electron microscopic immunocytochemistry and autoradiography. Virology **160:**220–226.
8. **Bienz, K., D. Egger, T. Pfister, and M. Troxler.** 1992. Structural and functional characterization of the poliovirus replication complex. J. Virol. **66:**2740–2747.
9. **Bienz, K., D. Egger, Y. Rasser, and W. Bossart.** 1983. Intracellular distribution of poliovirus proteins and the induction of virus-specific cytoplasmic structures. Virology **131:**39–48.
10. **Bienz, K., D. Egger, M. Troxler, and L. Pasamontes.** 1990. Structural organization of poliovirus RNA replication is mediated by viral proteins of the P2 genomic region. J. Virol. **64:**1156–1163.
11. **Blobel, G., and B. Dobberstein.** 1975. Transfer of proteins across membranes. I. Presence of proteolytically processed and unprocessed nascent immunoglobulin light chains on membrane-bound ribosomes of murine myeloma. J. Cell Biol. **67:**835–851.
12. **Blum, H., H. Beier, and H. J. Gross.** 1987. Improved silver staining of plant proteins, RNA and DNA in polyacrylamide gels. Electrophoresis **8:**93–99.
13. **Butterworth, B. E., E. J. Shimshick, and F. H. Yin.** 1976. Association of the polioviral RNA polymerase complex with phospholipid membranes. J. Virol. **19:**457–466.
14. **Caliguiri, L. A., and I. Tamm.** 1970. The role of cytoplasmic membranes in poliovirus biosynthesis. Virology **42:**100–111.
15. **Carlsson, S. R., J. Roth, F. Piller, and M. Fukuda.** 1988. Isolation and characterization of human lysosomal membrane glycoproteins, h-lamp-1 and h-lamp-2. Major sialoglycoproteins carrying polylactosaminoglycan. J. Biol. Chem. **263:**18911–18919.
16. **Cho, M. W., N. Teterina, D. Egger, K. Bienz, and E. Ehrenfeld.** 1994. Membrane rearrangement and vesicle induction by recombinant poliovirus 2C and 2BC in human cells. Virology **202:**129–145.
17. **Clark, M. E., T. Hämmerle, E. Wimmer, and A. Dasgupta.** 1991. Poliovirus proteinase 3C converts an active form of transcription factor IIIC to an inactive form: a mechanism for inhibition of host cell polymerase III transcription by poliovirus. EMBO J. **10:**2941–2947.
18. **Clark, M. E., P. M. Lieberman, A. J. Berk, and A. Dasgupta.** 1993. Direct cleavage of human TATA-binding protein by poliovirus protease 3C in vivo and in vitro. Mol. Cell. Biol. **13:**1232–1237.
19. **Crawford, N. A., A. Fire, M. Samuels, P. A. Sharp, and D. Baltimore.** 1981. Inhibition of transcription factor activity by poliovirus. Cell **27:**555–561.
20. **Dahl, R., and L. A. Staehelin.** 1989. High-pressure freezing for the preservation of biological structure: theory and practice. J. Electron Microsc. Tech. **13:**165–174.
21. **Dales, S., H. J. Eggers, I. Tamm, and G. E. Palade.** 1965. Electron microscopic study of the formation of poliovirus. Virology **26:**379–389.
22. **Dales, S., and R. M. Franklin.** 1962. A comparison of the changes in fine structure of L cells during single cycles of viral multiplication, following their infection with the viruses of mengo and encephalomyocarditis. J. Cell Biol. **14:**281–302.
23. **Datta, U., and A. Dasgupta.** 1994. Expression and subcellular localization of poliovirus VPg-precursor protein 3AB in eukaryotic cells: evidence for glycosylation in vitro. J. Virol. **68:**4468–4477.
24. **Ding, B. R., R. Turgion, and M. V. Parthasarathy.** 1991. Microfilament organization and distribution in freeze-substituted tobacco plant tissues. Protoplasma **165:**96–105.
25. **Doedens, J. R., and K. Kirkegaard.** 1995. Inhibition of cellular protein secretion by poliovirus proteins 2B and 3A. EMBO J. **14:**894–907.
26. **Dubois-Dalcq, M., K. V. Holmes, and B. Rentier.** 1984. Assembly of enveloped RNA viruses. Springer-Verlag, Vienna.
27. **Dunn, W. A., Jr.** 1990. Studies on the mechanisms of autophagy: formation of the autophagic vacuole. J. Cell Biol. **110:**1923–1933.
28. **Dunn, W. A., Jr.** 1990. Studies on the mechanisms of autophagy: maturation of the autophagic vacuole. J. Cell Biol. **110:**1935–1945.
29. **Dunn, W. A., Jr.** 1994. Autophagy and related mechanisms of lysosome-mediated protein degradation. Trends Cell Biol. **4:**139–143.
30. **Etchison, D., S. C. Milburn, I. Edery, N. Sonenberg, and J. W. B. Hershey.** 1982. Inhibition of HeLa cell protein synthesis following poliovirus infection correlates with the proteolysis of a 220,000-dalton polypeptide associated with eucaryotic initiation factor 3 and a cap binding protein complex. J. Biol. Chem. **257:**14806–14810.
31. **Franzusoff, A., E. Lauzé, and K. E. Howell.** 1992. Immunoisolation of Sec7p-coated transport vesicles from the yeast secretory pathway. Nature (London) **355:**173–175.
32. **Froshauer, S., J. Kartenbeck, and A. Helenius.** 1988. Alphavirus RNA replicase is located on the cytoplasmic surface of endosomes and lysosomes. J. Cell Biol. **107:**2075–2086.
33. **Gilkey, J. C., and L. A. Staehelin.** 1986. Advances in ultrarapid freezing for the preservation of cellular ultrastructure. J. Electron Microsc. Tech. **3:**177–210.
34. **Godman, G. C., R. A. Rifkind, C. Howe, and H. M. Rose.** 1964. A description of ECHO 9 virus infection in cultured cells. I. The cytopathic effect. Am. J. Pathol. **44:**1–27.
35. **Godman, G. C., R. A. Rifkind, R. B. Page, C. Howe, and H. M. Rose.** 1964. A description of ECHO 9 virus infection in cultured cells. II. Cytochemical observations. Am. J. Pathol. **44:**215–245.
36. **Goodarzi, M. T. G., and G. A. Turner.** 1994. Slot-blotting with enhanced chemiluminescence detection: an ultrasensitive technique for the quantita-

tive analysis of proteins and glycoproteins. Biochem. Soc. Trans. **22:**98S.
37. **Griffiths, G., M. Ericsson, J. Krijnse-Locker, T. Nilsson, B. Goud, H.-D. Söling, B. L. Tang, S. H. Wong, and W. Hong.** 1994. Localization of the Lys, Asp, Glu, Leu tetrapeptide receptor to the Golgi complex and the intermediate compartment in mammalian cells. J. Cell Biol. **127:**1557–1574.
38. **Griffiths, G., S. D. Fuller, R. Back, M. Hollinshead, S. Pfeffer, and K. Simons.** 1989. The dynamic nature of the Golgi complex. J. Cell Biol. **108:** 277–297.
39. **Guskey, L. E., P. C. Smith, and D. A. Wolff.** 1970. Patterns of cytopathology and lysosomal enzyme release in poliovirus-infected HEp-2 cells treated with either 2-(α-hydroxybenzyl)-benzimidazole or guanidine HCl. J. Gen. Virol. **6:**151–161.
40. **Harris, K. S., W. Xiang, L. Alexander, W. S. Lane, A. V. Paul, and E. Wimmer.** 1994. Interaction of poliovirus polypeptide 3CDpro with the 5′ and 3′ termini of the poliovirus genome. J. Biol. Chem. **269:**27004–27014.
41. **Heding, L. D., and D. A. Wolff.** 1973. The cytochemical examination of poliovirus-induced cell damage. J. Cell Biol. **59:**530–536.
42. **Hershman, K. M., W. W. Fleming, and D. A. Taylor.** 1993. A quantitative method for assessing protein abundance using enhanced chemiluminescence. Biotechniques **15:**790–796.
43. **Houri, J.-J., E. Ogier-Denis, G. Trugnan, and P. Codogno.** 1993. Autophagic degradation of N-linked glycoproteins is downregulated in differentiated human colon adenocarcinoma cells. Biochem. Biophys. Res. Commun. **197:** 805–811.
44. **Irurzun, A., J. Arroyo, A. Alvarez, and L. Carrasco.** 1995. Enhanced intracellular calcium concentration during poliovirus infection. J. Virol. **69:**5142–5146.
45. **Irurzun, A., L. Perez, and L. Carrasco.** 1992. Involvement of membrane traffic in the replication of poliovirus genomes: effects of brefeldin A. Virology **191:**166–175.
46. **Jezequel, A. M., and J. W. Steiner.** 1966. Some ultrastructural and histochemical aspects of Coxsackie-virus-cell interactions. Lab. Invest. **15:**1055–1083.
47. **Krijnse-Locker, J., M. Ericsson, P. J. M. Rottier, and G. Griffiths.** 1994. Characterization of the budding compartment of mouse hepatitis virus: evidence that transport from the rER to the Golgi complex requires only one vesicular transport step. J. Cell Biol. **124:**55–70.
48. **Laemmli, U. K.** 1970. Cleavage of structural proteins during the assembly of the head of bacteriophage T4. Nature (London) **227:**480–485.
49. **Lawrence, B. P., and W. J. Brown.** 1992. Autophagic vacuoles rapidly fuse with pre-existing lysosomes in cultured hepatocytes. J. Cell Sci. **102:**515–526.
50. **Lawrence, B. P., and W. J. Brown.** 1993. Inhibition of protein synthesis separates autophagic sequestration from the delivery of lysosomal enzymes. J. Cell Sci. **105:**473–480.
51. **Maynell, L. A., K. Kirkegaard, and M. W. Klymkowsky.** 1992. Inhibition of poliovirus RNA synthesis by brefeldin A. J. Virol. **66:**1985–1994.
52. **McBride, A. E., A. Schlegel, and K. Kirkegaard.** Identification of a human protein, Sam68, that interacts with poliovirus polymerase in infected cells. Proc. Natl. Acad. Sci. USA, in press.
53. **Moor, H.** 1987. Theory and practice of high pressure freezing, p. 175–191. *In* R. A. Steinbrecht and K. Zierold (ed.), Cryotechniques in biological electron microscopy. Springer-Verlag, Berlin.
54. **Pasamontes, L., D. Egger, and K. Bienz.** 1986. Production of monoclonal and monospecific antibodies against non-capsid proteins of poliovirus. J. Gen. Virol. **67:**2415–2422.
55. **Pata, J. D., S. C. Schultz, and K. Kirkegaard.** 1995. Functional oligomerization of poliovirus RNA-dependent RNA polymerase. RNA **1:**466–477.
56. **Pfister, T., D. Egger, and K. Bienz.** 1995. Poliovirus subviral particles associated with progeny RNA in the replication complex. J. Gen. Virol. **76:**63–71.
57. **Pfister, T., L. Pasamontes, M. Troxler, D. Egger, and K. Bienz.** 1992. Immunocytochemical localization of capsid-related particles in subcellular fractions of poliovirus-infected cells. Virology **188:**676–684.
58. **Punnonen, E.-L., S. Autio, H. Kaija, and H. Reunanen.** 1993. Autophagic vacuoles fuse with the prelysosomal compartment in cultured rat fibroblasts. Eur. J. Cell Biol. **61:**54–66.
59. **Rabouille, C., N. Hui, F. Hunte, R. Kieckbusch, E. G. Berger, G. Warren, and T. Nilsson.** 1995. Mapping the distribution of Golgi enzymes involved in the construction of complex oligosaccharides. J. Cell Sci. **108:**1617–1627.
60. **Rothman, J. E.** 1994. Mechanisms of intracellular protein transport. Nature (London) **372:**55–63.
61. **Rueckert, R. R.** 1990. Picornaviridae and their replication, p. 507–548. *In* B. N. Fields, D. M. Knipe, and R. M. Chanock (ed.), Virology 1. Raven Press, Ltd., New York.
62. **Schlegel, A., and K. Kirkegaard.** 1995. Cell biology of enterovirus infection, p. 135–154. *In* H. A. Rotbart (ed.), Human enterovirus infections. ASM Press, Washington, D.C.
63. **Schweizer, A., M. Ericsson, T. Bachi, G. Griffiths, and H. P. Hauri.** 1993. Characterization of a novel 63 kDa membrane protein. Implications for the organization of the ER-to-Golgi pathway. J. Cell Sci. **104:**671–683.
64. **Schweizer, A., J. Rohrer, J. W. Slot, H. J. Geuze, and S. Kornfeld.** 1995. Reassessment of the subcellular localization of p63. J. Cell Sci. **108:**2477–2485.
65. **Skinner, M. S., S. Halperen, and J. C. Harkin.** 1968. Cytoplasmic membrane-bound vesicles in echovirus 12-infected cells. Virology **36:**241–253.
66. **Strous, G. J., P. van Kerkhof, R. Willemsen, H. J. Geuze, and E. G. Berger.** 1983. Transport and topology of galactosyltransferase in endomembranes of HeLa cells. J. Cell Biol. **97:**723–727.
67. **Takeda, N., R. J. Kuhn, C.-F. Yang, T. Takegami, and E. Wimmer.** 1986. Initiation of poliovirus plus-strand RNA synthesis in a membrane complex of infected HeLa cells. J. Virol. **60:**43–53.
68. **Takegami, T., B. L. Semler, C. W. Anderson, and E. Wimmer.** 1983. Membrane fractions active in poliovirus RNA replication contain VPg precursor polypeptides. Virology **128:**33–47.
69. **Tershak, D. R.** 1984. Association of poliovirus proteins with the endoplasmic reticulum. J. Virol. **52:**777–783.
70. **Towbin, H., T. Staehelin, and J. Gordon.** 1979. Electrophoretic transfer of proteins from polyacrylamide gels to nitrocellulose sheets: procedure and some applications. Proc. Natl. Acad. Sci. USA **76:**4350–4354.
71. **Toyoda, H., C.-F. Yang, N. Takeda, A. Nomoto, and E. Wimmer.** 1987. Analysis of RNA synthesis of type 1 poliovirus by using an in vitro molecular genetic approach. J. Virol. **61:**2816–2822.
72. **Troxler, M., D. Egger, T. Pfister, and K. Bienz.** 1992. Intracellular localization of poliovirus RNA by in situ hybridization at the ultrastructural level using single-stranded riboprobes. Virology **191:**687–697.
73. **Trugnan, G., E. Ogier-Denis, C. Sapin, D. Darmoul, C. Bauvy, M. Aubery, and P. Codogno.** 1991. The N-glycan processing in HT-29 cells is a function of their state of enterocytic differentiation. Evidence for an atypical traffic associated with change in polypeptide stability in undifferentiated HT-29 cells. J. Biol. Chem. **266:**20849–20855.
74. **Watzele, G., R. Bachofner, and E. G. Berger.** 1991. Immunocytochemical localization of the Golgi apparatus using protein-specific antibodies to galactosyltransferase. Eur. J. Cell Biol. **56:**451–458.
75. **Wu, S.-X., P. Ahlquist, and P. Kaesberg.** 1992. Active complete in vitro replication of nodavirus RNA requires glycerophospholipid. Proc. Natl. Acad. Sci. USA **89:**11136–11140.